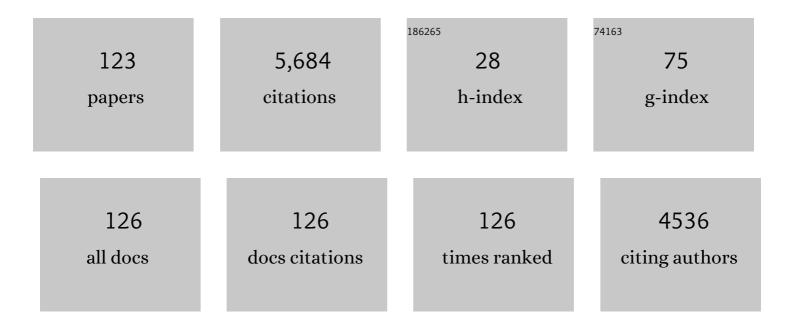
Yukihito Kondo

List of Publications by Year in descending order

Source: https://exaly.com/author-pdf/4858911/publications.pdf Version: 2024-02-01



#	Article	IF	CITATIONS
1	Controlling Depth Resolution of Phase Images by Ptychography using Achromatic Condition. Microscopy and Microanalysis, 2020, 26, 222-224.	0.4	0
2	Improvement of Spatial Resolution in Z Direction with Improved Energy Spread Measured using Aberration Corrected STEM with Cold Field Emission Gun. Microscopy and Microanalysis, 2019, 25, 514-515.	0.4	1
3	Investigation of Image Contrast in Biological Samples by Pixelated STEM Detector. Microscopy and Microanalysis, 2019, 25, 1694-1695.	0.4	0
4	Measuring Single Electrons – What Does it Mean?. Microscopy and Microanalysis, 2019, 25, 1654-1655.	0.4	1
5	Local Structural Study of Ferroelectric Domain Boundaries Using STEM-CBED with a Fast Pixelated STEM Detector. Microscopy and Microanalysis, 2019, 25, 1996-1997.	0.4	0
6	Strain measurement of a channel between Si/Ge stressors in a tri-gate field effect transistor utilizing moiré fringes in scanning transmission microscope images. Applied Physics Letters, 2019, 114, .	3.3	6
7	Morphology of phase-separated VO2 films deposited on TiO2-(001) substrate. Materials Research Bulletin, 2018, 102, 289-293.	5.2	7
8	Low Dose Imaging by STEM Ptychography Using Pixelated STEM Detector. Microscopy and Microanalysis, 2018, 24, 198-199.	0.4	4
9	Strain Analysis of FinFET Device Utilizing Moiré Fringes in Scanning Transmission Electron Microscopy. Microscopy and Microanalysis, 2018, 24, 978-979.	0.4	2
10	Energy Selected Secondary Electron Image Revealing Surface Potential by High Accelerating Voltage Scanning Electron Microscope. Microscopy and Microanalysis, 2018, 24, 1514-1515.	0.4	0
11	4D Analytical STEM with the pnCCD. Microscopy and Microanalysis, 2018, 24, 220-221.	0.4	1
12	Development of a secondary electron energy analyzer for a transmission electron microscope. Microscopy (Oxford, England), 2018, 67, 121-124.	1.5	1
13	Electron ptychographic phase imaging of light elements in crystalline materials using Wigner distribution deconvolution. Ultramicroscopy, 2017, 180, 173-179.	1.9	67
14	Advanced 4D STEM Imaging with the pnCCD (S)TEM Camera. Microscopy and Microanalysis, 2017, 23, 58-59.	0.4	0
15	Development of Fast Pixelated STEM Detector and its Applications using 4-Dimensional Dataset. Microscopy and Microanalysis, 2017, 23, 52-53.	0.4	8
16	Towards a Direct Visualization of Charge Transfer in Monolayer Hexagonal Boron Nitride using a Fast Pixelated Detector in the Scanning Transmission Electron Microscope. Microscopy and Microanalysis, 2017, 23, 436-437.	0.4	2
17	Way to Reduce Electron Dose in Pseudo Atomic Column Elemental Maps by 2D STEM Moire Method. Microscopy and Microanalysis, 2017, 23, 1790-1791.	0.4	4
18	Accelerating Voltage and Probe Current Dependence of Electron Beam Drilling Rates for Silicon Crystal. Microscopy and Microanalysis, 2017, 23, 1828-1829.	0.4	0

#	Article	IF	CITATIONS
19	Near Shadowless EDS Tomography for Sliced Sample Realized by X-ray Collection with One Large Sized SDD Detector. Microscopy and Microanalysis, 2017, 23, 1084-1085.	0.4	2
20	The Use of Electron Ptychography to Implement Efficient Phase Imaging in STEM. Microscopy and Microanalysis, 2016, 22, 466-467.	0.4	0
21	Effective Method for Decreasing Detection Limit of Dopant Concentration in Semiconductor Using Dual SDD Analysis System. Microscopy and Microanalysis, 2016, 22, 316-317.	0.4	0
22	Phase Imaging in STEM Allowing for Post-Acquisition Aberration Correction and 3D Optical Sectioning using Ptychography Wigner-Distribution Deconvolution. Microscopy and Microanalysis, 2016, 22, 508-509.	0.4	1
23	Pushing the Limits of Fast Acquisition in TEM Tomography and 4D-STEM. Microscopy and Microanalysis, 2016, 22, 512-513.	0.4	Ο
24	Pseudo Atomic Column EELS & EDS Mapping of Silicon Reconstructed With K and L Electrons Using STEM-Moiré Method. Microscopy and Microanalysis, 2016, 22, 264-265.	0.4	4
25	A pnCCD-based, fast direct single electron imaging camera for TEM and STEM. Journal of Instrumentation, 2016, 11, P04006-P04006.	1.2	97
26	Opportunities in Angularly Resolved Dark-field STEM using Pixelated Detectors. Microscopy and Microanalysis, 2015, 21, 2411-2412.	0.4	0
27	4D-STEM Imaging With the pnCCD (S)TEM-Camera. Microscopy and Microanalysis, 2015, 21, 2211-2212.	0.4	6
28	Atomic resolution ptychographic phase contrast imaging of polar-ordered structures in functional oxides. Microscopy and Microanalysis, 2015, 21, 1221-1222.	0.4	1
29	Rapid 3D Reconstruction in the EDS Tomography by using Iterative Series Reduction (ISER) Method. Microscopy and Microanalysis, 2015, 21, 1605-1606.	0.4	О
30	Development of Phase Contrast Scanning Transmission Electron Microscopy. Microscopy and Microanalysis, 2015, 21, 1943-1944.	0.4	1
31	Concentration at Detection Limit of Dopant for Semiconductor Samples Using Dual SDD Analysis System. Microscopy and Microanalysis, 2015, 21, 823-824.	0.4	2
32	Development of Phase Contrast Scanning Transmission Electron Microscopy and its application. Microscopy and Microanalysis, 2015, 21, 2301-2302.	0.4	1
33	High Efficiency Phase Contrast Imaging In STEM Using Fast Direct Electron Pixelated Detectors. Microscopy and Microanalysis, 2015, 21, 2303-2304.	0.4	3
34	Aberration Corrected Electron Microscopy Enhanced for Lower Accelerating Voltages. Microscopy and Microanalysis, 2015, 21, 1599-1600.	0.4	3
35	Phase-contrast scanning transmission electron microscopy. Microscopy (Oxford, England), 2015, 64, 181-187.	1.5	13
36	Magnified pseudo-elemental map of atomic column obtained by Moiré method in scanning transmission electron microscopy. Microscopy (Oxford, England), 2014, 63, 391-395.	1.5	20

#	Article	IF	CITATIONS
37	A Double Silicon Drift Type Detector System for EDS with Ultrahigh Efficiency and Throughput for TEM. Microscopy and Microanalysis, 2014, 20, 1150-1151.	0.4	15
38	Reproducible strain measurement in electronic devices by applying integer multiple to scanning grating in scanning moir $ ilde{A}$ © fringe imaging. AlP Advances, 2014, 4, 107107.	1.3	4
39	Direct observation of interstitial titanium ions in TiO2 substrate with gold nanoparticle. Surface Science, 2014, 619, 39-43.	1.9	9
40	First Demonstration of Phase Contrast Scanning Transmission Electron Microscopy. Microscopy and Microanalysis, 2014, 20, 224-225.	0.4	1
41	Accuracy of Strain in Strain Maps Improved by Averaging Multiple Maps. Microscopy and Microanalysis, 2014, 20, 1068-1069.	0.4	7
42	Image Collection using an Auto Data Acquisition System and An Application to Ice embedded Ribosome. Microscopy and Microanalysis, 2014, 20, 1114-1115.	0.4	0
43	Quantitative measurement of strain field in strained-channel-transistor arrays by scanning moir \tilde{A} © fringe imaging. Applied Physics Letters, 2013, 103, .	3.3	32
44	Strained hetero interfaces in Si/SiGe/SiGe/SiGe multi-layers studied by scanning moiré fringe imaging. Journal of Applied Physics, 2013, 114, .	2.5	21
45	Scanning moir \tilde{A} fringe imaging for quantitative strain mapping in semiconductor devices. Applied Physics Letters, 2013, 102, .	3.3	54
46	Channel-Length-Dependence of Strain Field in Transistor Studied via Scanning Moire Fringe Imaging. ECS Solid State Letters, 2013, 3, Q1-Q3.	1.4	7
47	Development of Cs and Cc correctors for transmission electron microscopy. Microscopy (Oxford,) Tj ETQq1 1	0.784 <u>31</u> 4 rg	BT/Overlock
48	Strain Analysis of Semiconductor Device by Moir \tilde{A} \mbox{C} Fringes in STEM Image. Microscopy and Microanalysis, 2013, 19, 346-347.	0.4	7
49	Compositional change of NaCl particles under electron beam irradiation measured by time-resolved X-ray analysis. Microscopy and Microanalysis, 2012, 18, 1052-1053.	0.4	2
50	Advantage of Cc/Cs-corrected Imaging in 30 kV Transmission Electron Microscopy. Microscopy and Microanalysis, 2012, 18, 1514-1515.	0.4	1
51	Element discrimination in a hexagonal boron nitride nanosheet by aberration corrected transmission electron microscopy. Ultramicroscopy, 2012, 122, 6-11.	1.9	2
52	Differential phase-contrast microscopy at atomic resolution. Nature Physics, 2012, 8, 611-615.	16.7	333
53	Surface Imaging by ABF-STEM: Lithium lons in Diffusion Channel of LIB Electrode Materials. E-Journal of Surface Science and Nanotechnology, 2012, 10, 454-458.	0.4	1
54	Innovative electron microscope for light-element atom visualization. Synthesiology, 2012, 4, 172-182.	0.2	2

#	Article	IF	CITATIONS
55	Experimental study of annular bright field (ABF) imaging using aberration-corrected scanning transmission electron microscopy (STEM). Micron, 2012, 43, 538-544.	2.2	71
56	Counting lithium ions in the diffusion channel of an LiV2O4 crystal. Journal of Applied Physics, 2011, 109, .	2.5	34
57	Aberration Correctors Developed Under the Triple C Project. Advances in Imaging and Electron Physics, 2011, 168, 297-336.	0.2	12
58	Reconstruction of Atomic Resolution STEM Images Using the Diffraction-Imaging Method with an Aberration-Corrected STEM. Microscopy and Microanalysis, 2011, 17, 1076-1077.	0.4	0
59	Performance and Application of an Aberration Corrected Analytical Electron Microscope with a Cold Field Emission Gun. Microscopy and Microanalysis, 2011, 17, 1162-1163.	0.4	1
60	Development of 30-kV Cc/Cs Correction Tandem System. Microscopy and Microanalysis, 2011, 17, 1184-1185.	0.4	1
61	A New Electron Microscope with an Easy Operation System for Nano Analysis. Microscopy and Microanalysis, 2011, 17, 1198-1199.	0.4	1
62	Direct Imaging of Hydrogen Atoms in a Crystal by Annular Bright-field STEM. Microscopy and Microanalysis, 2011, 17, 1278-1279.	0.4	0
63	Auto-Tuning of Aberrations Using High-Resolution STEM Images by Auto-Correlation Function. Microscopy and Microanalysis, 2011, 17, 1308-1309.	0.4	3
64	Performance and Application of Chromatic/Spherical Aberration-Corrected 30 kV Transmission Electron Microscope. Microscopy and Microanalysis, 2011, 17, 1530-1531.	0.4	3
65	Counting the Number of Lithium Atoms in the Diffusion Channel by Annular Bright Field imaging. Microscopy and Microanalysis, 2011, 17, 1580-1581.	0.4	Ο
66	Direct imaging of hydrogen-atom columns in a crystal by annular bright-field electron microscopy. Nature Materials, 2011, 10, 278-281.	27.5	313
67	Annular electron energy-loss spectroscopy in the scanning transmission electron microscope. Ultramicroscopy, 2011, 111, 1540-1546.	1.9	2
68	Quantitative annular dark-field STEM images of a silicon crystal using a large-angle convergent electron probe with a 300-kV cold field-emission gun. Journal of Electron Microscopy, 2011, 60, 109-116.	0.9	30
69	Visualization of Light Elements using Annular Bright Field Imaging with a Cs-corrected Scanning Transmission Electron Microscope. Journal of the Vacuum Society of Japan, 2011, 54, 248-252.	0.3	Ο
70	Atomic-Resolution STEM Imaging of Materials Using a Segmented Annular All Field Detector. Microscopy and Microanalysis, 2010, 16, 124-125.	0.4	1
71	Cross-section of Asbestos Prepared for TEM/STEM with Ion Slicer. Microscopy and Microanalysis, 2010, 16, 14-15.	0.4	1
72	Annular Bright Field Scanning Transmission Electron Microscopy Imaging Dynamics. Microscopy and Microanalysis, 2010, 16, 80-81.	0.4	11

#	Article	IF	CITATIONS
73	Development of a Segmented Detector for Aberration Corrected Scanning Transmission Electron Microscopes. Microscopy and Microanalysis, 2010, 16, 760-761.	0.4	0
74	Chromatic Aberration Correction by Combination Concave Lens. Microscopy and Microanalysis, 2010, 16, 116-117.	0.4	5
75	Higher-order aberration corrector for an image-forming system in a transmission electron microscope. Ultramicroscopy, 2010, 110, 958-961.	1.9	45
76	Oxygen-rich Ti1â^'O2 pillar growth at a gold nanoparticle–TiO2 contact by O2 exposure. Surface Science, 2010, 604, L75-L78.	1.9	18
77	Dynamics of annular bright field imaging in scanning transmission electron microscopy. Ultramicroscopy, 2010, 110, 903-923.	1.9	373
78	New area detector for atomic-resolution scanning transmission electron microscopy. Journal of Electron Microscopy, 2010, 59, 473-479.	0.9	118
79	Visualization of Lithium Atoms in LiV2O4 by a Spherical Aberration Corrected Electron Microscope. Microscopy and Microanalysis, 2010, 16, 162-163.	0.4	0
80	Visualization of Anitimony (Sb) Dopant Clusters in Silicon Specimen by Large Angle Convergent Beam HAADF-STEM. Microscopy and Microanalysis, 2010, 16, 1732-1733.	0.4	0
81	STEM imaging of 47-pm-separated atomic columns by a spherical aberration-corrected electron microscope with a 300-kV cold field emission gun. Journal of Electron Microscopy, 2009, 58, 357-361.	0.9	147
82	Electron Energy Loss Spectroscopy of Graphene Identified by Aberration, Corrected TEM at 300kV. Microscopy and Microanalysis, 2009, 15, 1484-1485.	0.4	3
83	Development of a multifunctional TEM specimen holder equipped with a piezodriving probe and a laser irradiation port. Journal of Electron Microscopy, 2009, 58, 245-249.	0.9	27
84	Correction of higher order geometrical aberration by triple 3-fold astigmatism field. Journal of Electron Microscopy, 2009, 58, 341-347.	0.9	70
85	Visualizing and identifying single atoms using electron energy-loss spectroscopy with low accelerating voltage. Nature Chemistry, 2009, 1, 415-418.	13.6	152
86	Robust atomic resolution imaging of light elements using scanning transmission electron microscopy. Applied Physics Letters, 2009, 95, .	3.3	334
87	Visualization of Light Elements at Ultrahigh Resolution by STEM Annular Bright Field Microscopy. Microscopy and Microanalysis, 2009, 15, 164-165.	0.4	181
88	Observation of Magnetic and Electric Field in STEM by using CCD camera. Microscopy and Microanalysis, 2009, 15, 1058-1059.	0.4	3
89	Development of a 200kV Atomic Resolution Analytical Electron Microscope. Microscopy and Microanalysis, 2009, 15, 188-189.	0.4	5
90	Correction of Spherical Aberration and Six-Fold Astigmatism Using Three Dodecapoles,. Microscopy and Microanalysis, 2009, 15, 1458-1459.	0.4	1

Үикініто Комдо

#	Article	IF	CITATIONS
91	Adatom on Graphene, Directly Imaged by Aberration Corrected TEM at 300kV. Microscopy and Microanalysis, 2009, 15, 1476-1477.	0.4	1
92	In-Situ Observation of Au/TiO2 Catalyst in Oxygen-Gas Environments. Microscopy and Microanalysis, 2009, 15, 692-693.	0.4	0
93	TEM and STEM Tomography for thick polymer sample. Microscopy and Microanalysis, 2009, 15, 630-631.	0.4	1
94	Highly Stable 300kV Cold Field Emission Gun for 50pm Resolution Electron Microscopy. Microscopy and Microanalysis, 2009, 15, 1084-1085.	0.4	2
95	Performance of Low-voltage Electron Microscope with New Aberration Correction System and Cold Field Emission Gun. Microscopy and Microanalysis, 2009, 15, 1080-1081.	0.4	Ο
96	Detection of Arsenic Dopant Atoms in Silicon Crystal by Aberration Corrected Scanning Transmission Electron Microscope. Microscopy and Microanalysis, 2009, 15, 1488-1489.	0.4	0
97	Measurement method of aberration from Ronchigram by autocorrelation function. Ultramicroscopy, 2008, 108, 1467-1475.	1.9	78
98	Atomic Resolution Elemental Maps by Core Level EELS Using Cs Corrected STEM. Microscopy and Microanalysis, 2008, 14, 1372-1373.	0.4	2
99	Development of Double-Probe Piezo-Driving Holder for TEM. Microscopy and Microanalysis, 2008, 14, 814-815.	0.4	0
100	Auto-Adjustment of Aberration Correction and Experimental Evaluation of R005 Microscope. Microscopy and Microanalysis, 2008, 14, 802-803.	0.4	1
101	Development of Domestic Spherical Aberration Correction Electron Microscope, R005. Journal of the Vacuum Society of Japan, 2008, 51, 714-718.	0.3	1
102	Achieving 63 pm Resolution in Scanning Transmission Electron Microscope with Spherical Aberration Corrector. Japanese Journal of Applied Physics, 2007, 46, L568-L570.	1.5	62
103	The Development of Ultra-high Vacuum Cs-Corrected Scanning Transmission Electron Microscope for Fast Fabrication of Desired Nanostructures. Microscopy and Microanalysis, 2006, 12, 1366-1367.	0.4	2
104	Atomic Resolution Elemental Map of EELS with a Cs Corrected STEM. Microscopy and Microanalysis, 2006, 12, 1150-1151.	0.4	30
105	Simultaneous measurements of conductivity and magnetism by using microprobes and electron holography. Applied Physics Letters, 2006, 88, 223103.	3.3	27
106	In-situ UHV-Electron Microscopy with Scanning Tunneling Microscope. Microscopy and Microanalysis, 2002, 8, 414-415.	0.4	0
107	A New High-Resolution Electron Microscope with Easy Operation System for Nano Analysis. Microscopy and Microanalysis, 2002, 8, 1106-1107.	0.4	0
108	Observation of device cross-sectional thin films prepared by FIB using JEM-2500SE, an electron microscope for nano-analysis. Microscopy and Microanalysis, 2002, 8, 1176-1177.	0.4	0

#	ARTICLE	IF	CITATIONS
109	Ultrahigh-Vacuum Electron Microscopy for Gold Nanostructures. Microscopy and Microanalysis, 2001, 7, 920-921.	0.4	0
110	Quantitative high-resolution microscopy on a suspended chain of gold atoms. Ultramicroscopy, 2001, 88, 17-24.	1.9	41
111	Synthesis and Characterization of Helical Multi-Shell Gold Nanowires. Science, 2000, 289, 606-608.	12.6	724
112	Three-Horned Multishell Fullerene. Japanese Journal of Applied Physics, 1999, 38, L1208-L1210.	1.5	0
113	Thickness Induced Structural Phase Transition of Gold Nanofilm. Physical Review Letters, 1999, 82, 751-754.	7.8	87
114	Quantized conductance through individual rows of suspended gold atoms. Nature, 1998, 395, 780-783.	27.8	1,325
115	UHV electron microscope and simultaneous STM observation of gold stepped surfaces. Surface Science, 1998, 415, L1061-L1064.	1.9	25
116	Vacuum Nanotechnology. Synthesis of New Materials and Characterization of Surfaces and Interfaces. Observation of Gold Atom Bridge by Ultrahigh Vacuum Transmission Electron Microscope Shinku/Journal of the Vacuum Society of Japan, 1998, 41, 917-920.	0.2	0
117	Atom-Bridge to Nano-Wire. Microscopy and Microanalysis, 1997, 3, 391-392.	0.4	0
118	Procedure to Determine the Structure of Three-Horned Multishell Fullerene. Microscopy and Microanalysis, 1997, 3, 419-420.	0.4	0
119	Gold Nanobridge Stabilized by Surface Structure. Physical Review Letters, 1997, 79, 3455-3458.	7.8	368
120	Attraction and orientation phenomena of bucky onions formed in a transmission electron microscope. Chemical Physics Letters, 1996, 259, 425-431.	2.6	47
121	Design and development of an ultrahigh vacuum high-resolution transmission electron microscope. Ultramicroscopy, 1991, 35, 111-118.	1.9	42
122	Design features of an ultrahigh-vacuum electron microscope for REM-PEEM studies of surfaces. Ultramicroscopy, 1991, 36, 142-147.	1.9	23
123	New Electron Diffraction Techniques Using Electronic Hollow-Cone Illumination. Japanese Journal of Applied Physics, 1984, 23, L178-L180.	1.5	18